



# Characteristics of pipe corrosion scales in untreated water distribution system and effect on water quality in Peshawar, Pakistan

Dilawar Farhan Shams<sup>1</sup> · Saeed Islam<sup>1</sup> · Baoyou Shi<sup>2</sup> · Waliullah Khan<sup>3</sup> · Buddhika Gunawardana<sup>4</sup> · Maryam Saad<sup>1</sup> · Muhammad Qasim<sup>1</sup> · Haider Ali Javed<sup>1</sup> · Sahib Gul Afridi<sup>5</sup> · Muhammad Naeem<sup>3</sup> · Gul Shahzada Khan<sup>3</sup>

Received: 28 October 2018 / Accepted: 27 December 2018 / Published online: 6 January 2019  
© Springer-Verlag GmbH Germany, part of Springer Nature 2019

## Abstract

This study investigated the characteristics of iron corrosion scales in pipes at tube well, overhead tank, and consumers' end in older untreated water distribution system in Peshawar city, Pakistan. Effect of water quality conditions on corrosion scales and that of scales on drinking water quality in such systems was also assessed by undertaking a comparison with new piped distribution systems. The scales were analyzed for chemical composition and morphology using X-ray diffraction (XRD), inductively coupled plasma (ICP), and a scanning electron microscope (SEM), while water quality was examined for physico-chemical and biological characteristics. The main crystalline phases of corrosion scales were goethite, magnetite, siderite, and quartz. From tube well to consumers' end, goethite increased from 36 up to 48%, quartz declined from 22 to 15%, while magnetite fluctuated and siderite disappeared. Elemental composition of scales showed the deposition of Zn, Al, Mn, Cr, Pb, Cu, As, and Cd with Zn (13.9 g/kg) and Al (3.6 g/kg) in highest proportion. The SEM analysis illustrated the presence of microbial communities indicating the formation of biofilms in the corrosion scales. The significant difference ( $P < 0.05$ ) in levels of dissolved oxygen (DO),  $\text{Cl}^-$ ,  $\text{SiO}_4^{4-}$ , electrical conductivity (EC),  $\text{SO}_4^{2-}$ ,  $\text{NO}_3^-$ , alkalinity, hardness, and trace metals between old (DS-O) and new piped systems indicated their role in corrosion scale formation/destabilization and the effect of scale dissolution on water quality. In DS-O, EC, Cu, and Mn were significantly higher ( $P < 0.05$ ), whereas turbidity, EC, DO, and  $\text{SiO}_4^{4-}$  significantly increased from source to consumers' end implying a higher dissolution of scales and lowered corrosion rates in DS-O to utilize  $\text{SiO}_4^{4-}$  and DO for iron oxidation.

**Keywords** Corrosion scales · Drinking water · Water quality · Composition · Dissolution · Microorganisms

---

Dilawar Farhan Shams and Saeed Islam contributed equally to this work.

Responsible editor: Philippe Garrigues

---

✉ Dilawar Farhan Shams  
drfarhan@awkum.edu.pk

<sup>1</sup> Department of Environmental Sciences, Abdul Wali Khan University Mardan, Mardan 23200, Pakistan

<sup>2</sup> Research Center for Eco-Environmental Sciences, Chinese Academy of Sciences, Beijing 100085, China

<sup>3</sup> Department of Chemistry, Abdul Wali Khan University Mardan, Mardan 23200, Pakistan

<sup>4</sup> Department of Civil Engineering, University of Moratuwa, Moratuwa 10400, Sri Lanka

<sup>5</sup> Department of Biochemistry, Abdul Wali Khan University Mardan, Mardan 23200, Pakistan

## Introduction

Corrosion scale formation in iron pipes used in drinking water distribution systems is a common issue faced by municipal authorities aiming to ensure regular and clean supply of potable water to the consumers. This issue is of more concern in old distribution networks having extensively used pipes for years with substantial deposits of scales. In water pipes, corrosion scales and tubercles restrict the hydraulic flow; impair water quality; increase the demand for chlorine, dissolved oxygen (DO), and energy for water delivery; promote microbial growth in biofilms; accumulate toxic chemicals such as arsenic and other heavy metals; and release iron particles leading to colored water (Chaves and Manuel 2013; Sarin et al. 2004b).

Formation of corrosion scales in pipes is a natural phenomenon that mainly occurs due to reaction of oxygen in water with metals like iron. Principally, the scales are composed of

goethite, magnetite, lepidocrocite, siderite, ferrous hydroxide, ferric hydroxide, ferrihydrite, green rust, and calcium carbonate (Benjamin et al. 1996). When drinking water pipes are used for several years, corrosion scales deposit over the inner walls of the pipes. The deposited layers consist of a corroded metal floor, a porous inner core layer, and a loosely accumulated layer on solid-liquid interface (Li et al. 2016a). The composition and rate of corrosion depends upon several factors such as the type of pipe inner material, temperature variations, water flow in pipes, and microbial growth; however, water quality conditions also play a key role.

Several water quality constituents have been reported to influence corrosion such as alkalinity, dissolved oxygen (DO), pH, hardness, natural organic matter, and chlorides (Sarin et al. 2004b). Water may also contain dissolved ions that react with the pipe material and causes its decomposition (McFarland et al. 2008). Similarly, water quality also affects the deposition of metals and their dissolution in water, thereby inducing chemical transformation (Gonzalez et al. 2013). Meanwhile, drinking water is mandatorily treated in developed countries by employing physical/chemical treatment and disinfection processes. As a result, chemical, biological, and aesthetic characteristics of water are changed to make it more acceptable with removal of colloidal matter, hardness, and microbes for instance. In Pakistan, water supply systems are poorly managed with general lack of treatment, faulty distribution systems, cross-connections with sewerage lines and sewage drains, and leaked or damaged pipes that result in poor quality of drinking water (Altaf et al. 1993). The resulting water quality due to such conditions may play a major role in altering the composition and rate of corrosion scales, which may be different at various points in the distribution system such as at the source, overhead tank (OHT), and consumers' end depending on the specific conditions. Moreover, pipes are replaced after longer periods of time, usually 25 to 30 years. This may lead to extensive deterioration of pipes and formation of thick scales to impair water quality and cause serious health risks (Aziz 2005). On the other hand, corrosion scale products may also induce a change in water quality characteristics such as alkalinity, hardness, DO, pH, and buffer intensity and serve as a niche for the growth of microorganisms causing biological contamination of water (McNeill and Edwards 2001; Yang et al. 2012). Similarly, metals such as Cd, Fe, Pb, Cu, Al, Zn, and Cr may leach from the pipe scales and materials into flowing water (Gonzalez et al. 2013). Hence, the interaction of water with corrosion scales and tubercles might significantly affect the water quality characteristics in pipes.

While corrosion scales in water distribution pipes have been studied before, scale composition and consequent effect on water quality at different points in the absence of

drinking water treatment in poorly managed distribution systems has received less attention. The purpose of this study was to find and compare the characteristics of corrosion scales in pipes carrying untreated water in an older distribution system at the tube well (source), OHT, and consumers' end points. The study also aimed to assess the effect on water quality in such systems from the source to consumers' end in comparison to distribution systems with newly installed pipes.

## Materials and methods

### Study area and sampling

The study was conducted in District Peshawar, the capital of Khyber Pakhtunkhwa Province in the northwest Pakistan. Peshawar is located at 34° 02' N, 71° 37' E having an area of 1257 km<sup>2</sup> and population of 4.27 million with a population density of 3396 km<sup>2</sup> (PBS 2017). Public water supply is mainly withdrawn from groundwater sources. In most parts of the city, water is supplied untreated without any filtration or disinfection. The pipes are laid haphazardly with 37% above ground often across/along open sewage drain and made of galvanized iron (GI, 65%), PVC (21%), and asbestos cement (13%) (USAID 2014).

For characterization of corrosion scales, samples of pipe sections were obtained from a distribution system (with untreated groundwater source) undergoing replacement (Fig. 1). Pipe sections (76 cm in length) were obtained each from the source (tube well pipe), overhead tank (OHT) (from outflow pipe), and distribution system (consumers' end) that were all made of galvanized iron and installed 25 to 30 years ago (USAID 2014). The corrosion scales were extracted for analysis according to Li et al. (2016b). For drinking water quality assessment, samples were collected from three drinking water distribution systems in the same area (Fig. 1) following standard protocols as described in Khan et al. (2013). The first distribution system (DS-O) had older pipes of the same age as the one sampled for corrosion scales in the same vicinity while the two other systems (DS-N1) and (DS-N2) had newly installed pipes. Due to absence of OHT in most water distribution systems in the city including DS-N1 and DS-N2, samples were collected only from the source (tube well) and consumers' end to compare water quality status in the three systems.

### Crystalline phase composition of corrosion scales

Crystalline matter of the scale samples was analyzed by X-ray diffraction (XRD, PANalytical X'Pert PRO MPD). The scale samples were first grounded with agate mortar and

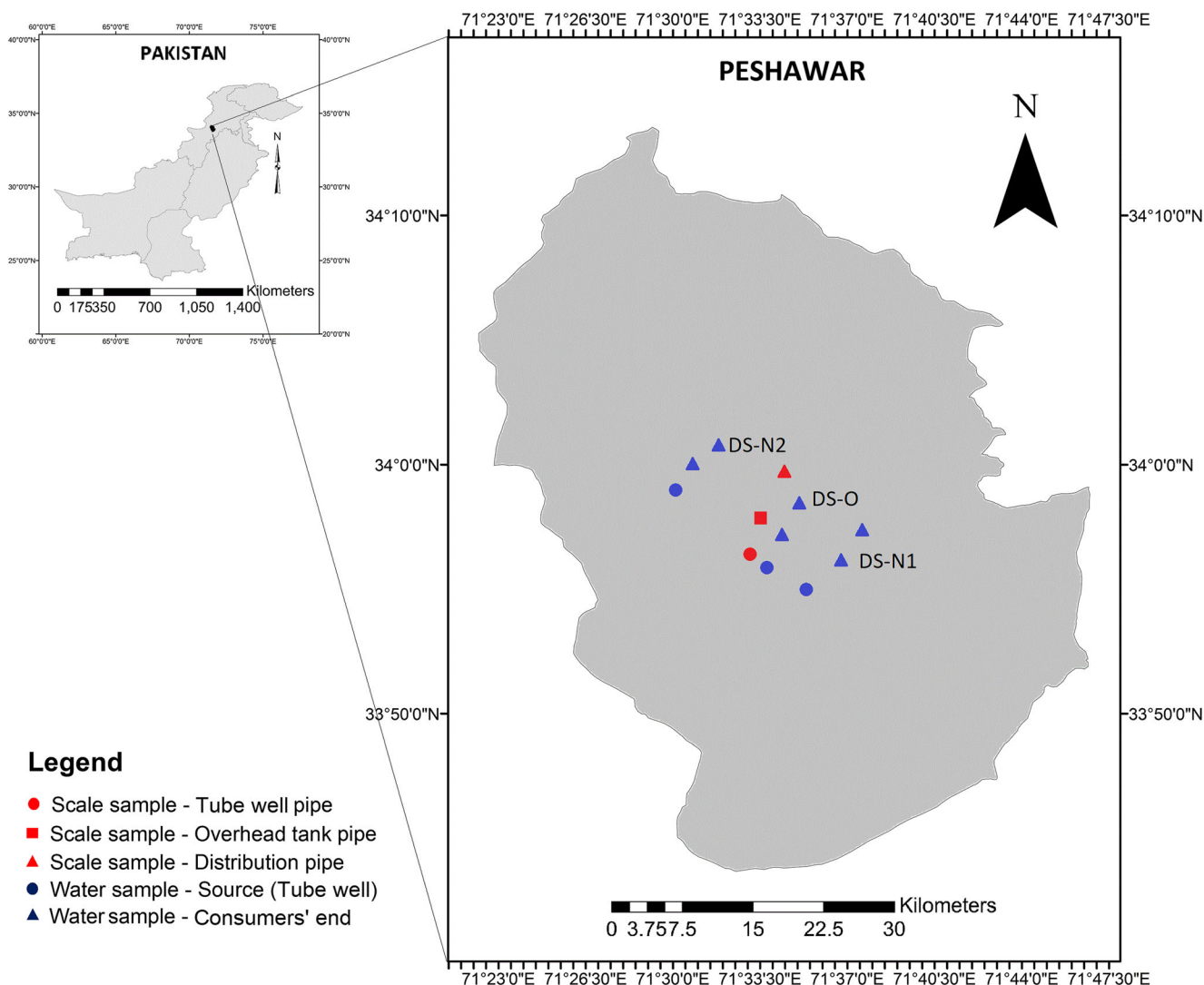


Fig. 1 Location of sampling points in the study area

pestle in anaerobic condition and then sieved out using a 1600- $\mu\text{m}$  mesh. The XRD operational parameters were Ni-filtered Cu-K $\alpha$  radiation ( $\lambda$  of 1.5406Å); the range of 2 $\theta$  values 3–70° with a 0.02° step size. Crystalline phase was identified using the Jade XRD software and crystalline phase composition was determined quantitatively by contrasted parameters of intensity method (Li et al. 2016b).

### Elemental composition of corrosion scales

Elemental composition of scales was analyzed using plasma mass spectrometry. The scale samples were first digested by adjusting the pH to less than 2.0 with concentrated nitric acid. Aluminum (Al), chromium (Cr), manganese (Mn), zinc (Zn), arsenic (As), cadmium (Cd), lead (Pb), and copper (Cu) were analyzed using inductively coupled plasma mass spectrometry (ICP-PMS, NexION 300X, PerkinElmer, USA (Peng et al. 2010)).

### Scanning electron microscopy of corrosion scales

Scanning electron microscopy (SEM) was performed to examine the morphology of corrosion scales for the presence of microorganisms using a Jeol 5910 scanning electron microscope. The samples were first dehydrated using 50%, 70%, 95%, and 100% ethanol concentration and then subjected to high concentration of amyl acetate to remove the ethanol impurities (Miller et al. 2005). The specimens were then mounted with silver collodion adhesive to an aluminum mounted stub. The samples were then coated with gold palladium metal and observed under SEM.

### Water quality analysis

Water samples were analyzed for physicochemical characteristics and total coliform bacteria. For pH, electrical conductivity (EC) and turbidity measurements, inoLab pH meter

(Model pH 7110), HACH conductivity meter (DR/3 spectrophotometer), and HACH turbidity meter (Model 2100A) were used respectively (HACH 2002). Alkalinity and total hardness were measured following HACH methods 8203, 10247, and 8149 respectively (HACH 2002). For nitrates (NO<sub>3</sub><sup>-</sup>), nitrites (NO<sub>2</sub><sup>-</sup>), chlorides (Cl<sup>-</sup>), sulfates (SO<sub>4</sub><sup>2-</sup>), and dissolved oxygen (DO), standard methods 4500-NO<sub>3</sub><sup>-</sup> C, 4500-NO<sub>2</sub><sup>-</sup> B, 4500-Cl<sup>-</sup> D, 4500-SO<sub>4</sub><sup>2-</sup> D, and 4500-O C were used respectively (APHA 2012). Levels of these physicochemical parameters found in the old and new distribution systems have been shown in Table 1. Total coliform bacteria were determined using multiple tube dilution method (Harris et al. 2012). Among heavy metals, Mn, Cu, and Cr were analyzed using atomic absorption spectrophotometry (Hitachi-Z-2000).

**Statistical analysis**

Standard deviations have been used to indicate variation in observed values. For comparison of water quality concentrations at source (tube well) and consumers’ end in the distribution systems, significance tests were performed using two-way ANOVA with IBM-SPSS version 22.0 (2013). Multiple pairwise comparisons were also carried out for the marginal means for significant main and interaction effect using the Sidak method. For significant results, a *P* < 0.05 was used.

**Results and discussion**

**Crystalline phase composition of corrosion scales**

The XRD patterns showed that the main constituents of scales in pipes from the source (tube well), OHT, and consumers’ end were goethite (α-FeOOH), magnetite (Fe<sub>3</sub>O<sub>4</sub>), and quartz (SiO<sub>2</sub>). Siderite (FeCO<sub>3</sub>) was observed only in tube well and overhead pipes (Fig. 2). Goethite was found

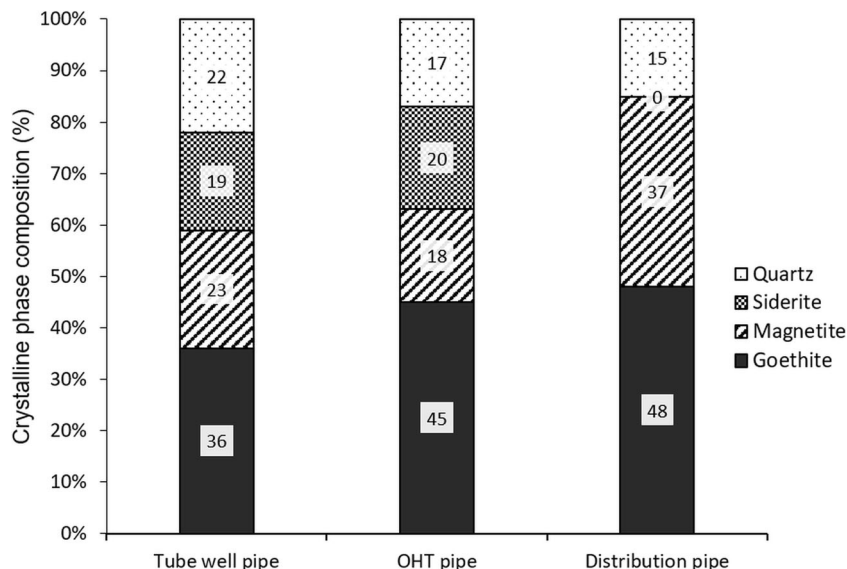
in relatively higher proportions and showed a general increase from tube well to distribution pipes. Dissolved oxygen (DO) seemed to have caused this increase as it induces the conversion of Fe<sup>2+</sup> to Fe<sup>3+</sup>, which in turn increases the chances of goethite formation (Benson 2009). DO was present in the source water as found in the distribution system with old pipes (DS-O) and increased from 4.4 ± 0.2 to 6 ± 0.5 mg/L in the distribution lines most likely due to aeration in the overhead tank (7.4 ± 0.3 mg/L). DO also seems to have played a role in increasing the magnetite content in the distribution pipe to 37% from 18% in the overhead tank pipe through oxidation of the ferrous ions (Drissi et al. 1995). Magnetite is among the more stable phases that are formed at low oxidation rates of Fe (II) inside the scales (Sarin et al. 2004b). Besides DO, anions such as Cl<sup>-</sup>, SO<sub>4</sub><sup>2-</sup>, and NO<sub>3</sub><sup>-</sup> may also have contributed to the formation of magnetite as they affect the scale composition as well as the corrosion rates through complexation with dissolved iron (Tamura et al. 1981). Moreover, formation of both magnetite and goethite has also been linked to the relevant biochemical functions of bacterial community found in corrosion scales such as iron- and sulfur-oxidizing bacteria and iron-, sulfate-, and nitrate-reducing bacteria (Wang et al. 2017). Siderite content was nearly the same in both the tube well and overhead tank pipes but absent in the distribution line which is mainly caused by the oxidation of siderite to magnetite. Quartz fraction was higher in the source pipes, which points to the carryover of sand from the untreated source water (Copeland et al. 2007).

For crystalline composition in GI pipe scales with treated groundwater, Zhang et al. (2008) observed magnetite as the main crystalline ferrous compound and also found goethite, hematite (Fe<sub>2</sub>O<sub>3</sub>), and elemental Fe. Tang et al. (2006) found akaganeite (β-FeOOH) and ZnO as the major crystalline phases and also observed hematite and magnetite. Others have

**Table 1** Mean concentration of physicochemical parameters in water distribution systems (SD in parenthesis)

Parameters	DS-O (old)		DS-N1 (new)		DS-N2 (new)	
	Tube well	Consumers’ end	Tube well	Consumers’ end	Tube well	Consumers’ end
Alkalinity (mg/L)	280 (2)	260 (12)	300 (3)	281 (10)	281 (3)	300 (11)
Turbidity (NTU)	1.6 (0.1)	2.8 (0.2)	3.5 (0.1)	1.6 (0.2)	1.5 (0.1)	1.7 (0.1)
Hardness (mg/L)	370 (3)	424 (5)	470 (3)	400 (66)	430 (2)	460 (11)
EC (µS/cm)	371 (2)	404 (2)	368 (4)	372 (3)	371 (2)	374 (2)
pH	7.7 (0.0)	7.4 (0.2)	7.2 (0.0)	7.3 (0.1)	7.2 (0.0)	7.4 (0.1)
Chlorides (mg/L)	55.3 (2.1)	60.5 (5.8)	55.0 (1.0)	39.2 (6.9)	53.3 (2.1)	37.0 (6.6)
Sulfates (mg/L)	52.3 (2.1)	50.2 (1.7)	57.0 (1.0)	52 (1.9)	54.7 (1.5)	52.2 (2.6)
Nitrates (mg/L)	1.2 (0.2)	6.5 (0.5)	8.9 (0.2)	6.5 (0.2)	1.2 (0.1)	1.5 (0.2)
DO (mg/L)	4.5 (0.3)	6.0 (0.5)	4.5 (0.1)	4.1 (0.3)	3.4 (0.2)	3.6 (0.2)
Silicates (mg/L)	1.6 (0.1)	2.8 (0.2)	3.5 (0.1)	1.6 (0.2)	1.5 (0.1)	1.7 (0.1)

**Fig. 2** Crystalline phase composition of corrosion scales

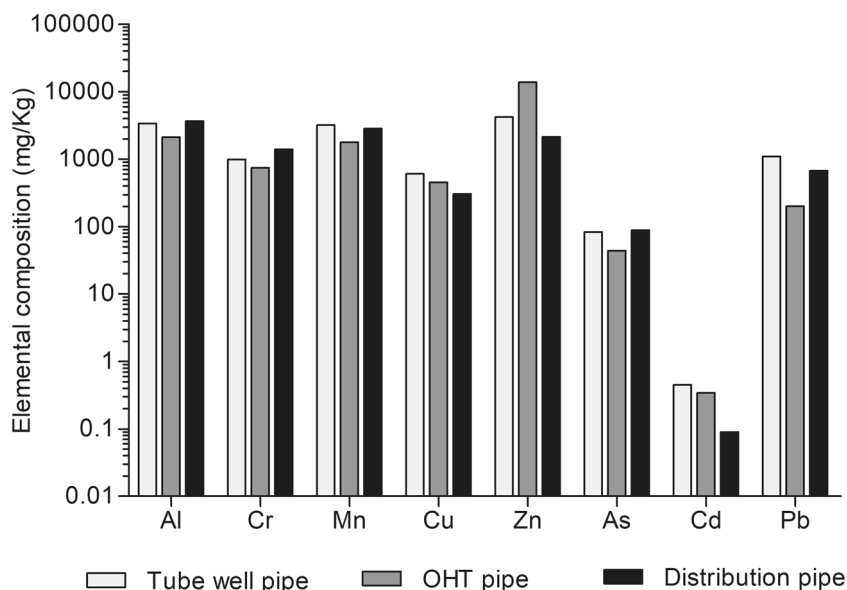


also reported the presence of lepidocrocite ( $\gamma\text{-FeOOH}$ ), maghemite ( $\gamma\text{-Fe}_2\text{O}_3$ ), and calcite ( $\text{CaCO}_3$ ) as well as hydrotalcite-like compounds in some cases (Borch et al. 2008; Li et al. 2016a; Liu et al. 2015; Tang et al. 2006; Zhang et al. 2008). The types and content of crystalline compounds varied, which is usually attributed to water source, hydraulic conditions, and pipe age (Liu et al. 2015; Yang et al. 2012). In this study, the crystalline composition depicted a different scenario with the observed four phases and the variation in their contents at different points in the distribution system. Goethite and magnetite were the predominant crystalline phases and their combined fraction increased from 59% at tube well to 85% in the distribution pipe. Also noticeable was the higher content of quartz in scales especially in the tube well pipe that directly points to the effect of untreated source water.

**Elemental composition of scales**

Elemental composition of scales showed the presence of major metallic elements as well as toxic contaminants in the order: tube well ( $\text{Zn} > \text{Al} > \text{Mn} > \text{Pb} > \text{Cr} > \text{Cu} > \text{As} > \text{Cd}$ ), overhead tank ( $\text{Zn} > \text{Al} > \text{Mn} > \text{Cr} > \text{Cu} > \text{Pb} > \text{As} > \text{Cd}$ ), and distribution system ( $\text{Al} > \text{Mn} > \text{Zn} > \text{Cr} > \text{Pb} > \text{Cu} > \text{As} > \text{Cd}$ ). The deposition and abundance of these constituents in scales was dependent on the water quality and morphological conditions in pipes and corrosion scale composition. In the study area, presence of these constituents in drinking water has been reported in various studies (Bacha et al. 2010; Khan et al. 2016) that may be one of the contributors to their occurrence in scales. From the elemental composition, Zn and Al were the most abundant (Fig. 3). The accumulation of relatively higher

**Fig. 3** Elemental composition of scales in tube well, overhead tank, and distribution pipes (shown in log-scale)





amount of Zn especially in tube well and overhead tank pipes may have resulted from the galvanization layer on the pipe having a Zn coat to prevent rusting (Sarin et al. 2001). Al together with Cr and As exhibited a similar trend with a decline in overhead tank from the source and then increase in the distribution pipe (Fig. 3). Al and Cr have been reported to mainly come from the use of cement mortar lining in pipes (Gonzalez et al. 2013). In the studied distribution systems, such linings were not used. Taps and metallic part portions may also be one of the source (Veschetti et al. 2010); however, presence of these heavy metals in scales could be tracked to the source water from where they enter in trace quantities but accumulate in corrosion scales in amounts exceeding those in water by several order of magnitude (Peng and Korshin 2011). The accumulation is augmented by the presence of various iron oxides such as goethite and magnetite that have strong potential to adsorb and assemble these and other trace heavy metals in corrosion scales (Peng et al. 2010; Sarin et al. 2001; Sun et al. 2017). In scales, Al content can be affected by chlorides in water having an inverse relationship (Wang et al. 2011). Chloride concentrations in water showed a correspondingly opposite trend at the three points in DS-O as shown in Table 1 below. In case of Cr, the fluctuations could be linked to magnetite in scales that upon decomposition releases ferrous ion, which reacts with Cr and reduces its concentration (Sedlak and Chan 1997). Meanwhile, As is released from aquifers from the desorption of As adsorbed on mineral oxides (mainly Fe, Mn, and Al oxides) that is enhanced in the presence of silicate, bicarbonate, phosphate, and organic matter (Smedley and Kinniburgh 2002). In scales, As accumulation has been reported to strongly correlate with Al concentration due to adsorption of As by the aluminosilicate phase essentially at neutral pH (Kim and Herrera 2010), as was the case in this study. Also, variation in As content in scales at the different distribution points may be affected by the corresponding chloride concentrations reacting with free iron to form  $\text{FeCl}_3$  that acts as absorbent (Jeong 2005).

Mn and Pb showed a decrease from source to overhead tank pipes and then increased in the distribution again. Mn concentration might have reduced due to retention in the overhead tank, whereas Pb deposition in scales could be affected by various factors such as pH, alkalinity, and water flow (Copeland et al. 2007). Nevertheless, further increase in both Mn and Pb in the distribution pipes indicated contamination in leaked sections of the pipes (Barbeau et al. 2011). For Cu and Cd, concentrations decreased from source to overhead and distribution pipes. The decrease in Cu levels may be explained by the presence of Cu-reducing bacteria in the untreated water that may use Cu and prevent it from deposition (Fish et al. 2016). The presence of bacteria was confirmed by the total coliform bacteria in DS-O as 240, 540, and 1600 MPN/100 ml in tube well, overhead, and distribution points respectively. A decline in Cd may be caused by water stagnation in pipes and

the hardness and chloride levels (Barton 2005). In comparison to distribution systems with GI pipes of the same age and treated water (Liu et al. 2015), the fraction of metals deposited in scales in this study was higher up to 2×, 52×, 1.6×, 22×, 25×, and 15× for Al, Cr, Mn, Cu, Zn, and Pb respectively. With similar pipe material (GI), the comparatively higher proportions of trace metals in scales may be linked to the untreated bulk water (and the accompanying suspended matter) flowing through the pipes from where these metals are retained and accumulated over a longer period of time through bio-adhesion, sorption, chemical bonding, and settling (Liu et al. 2017).

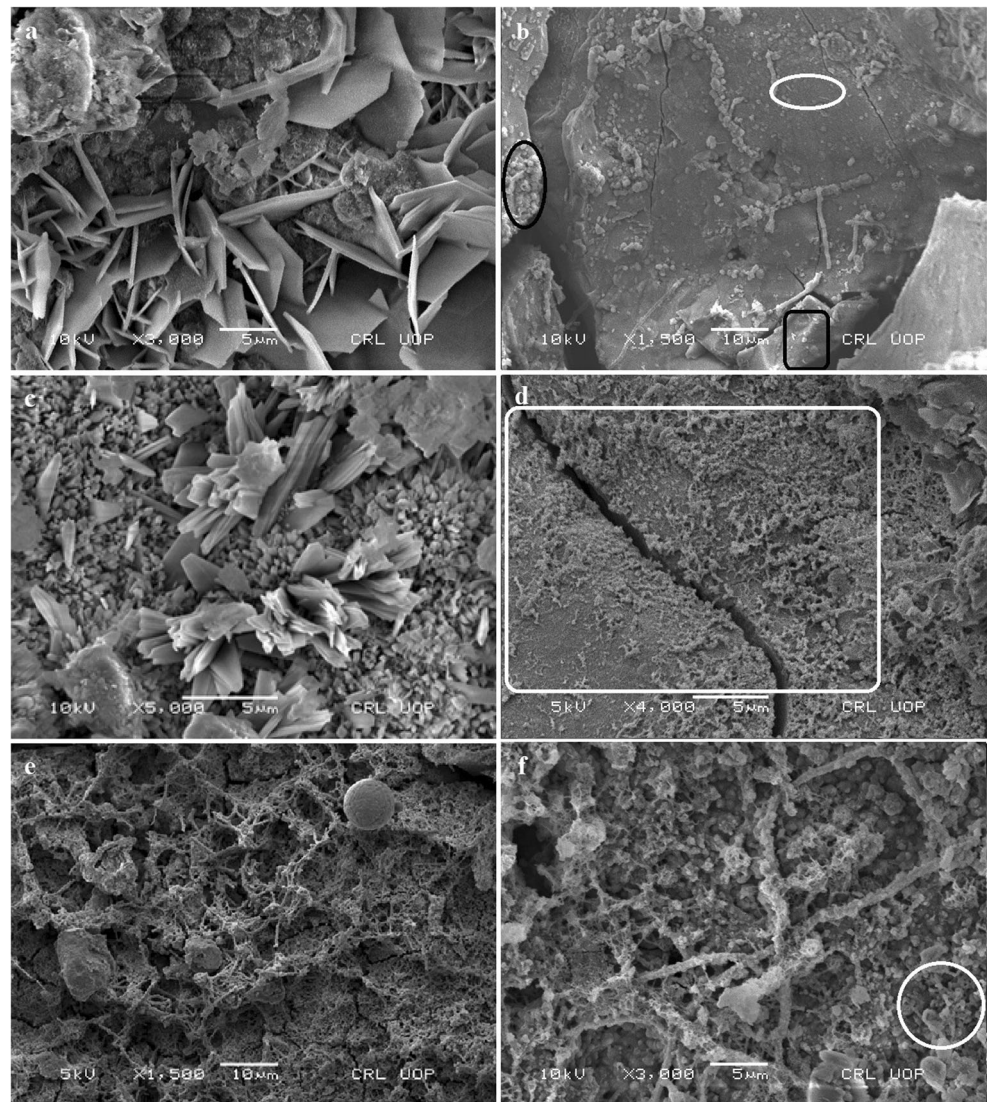
### SEM of corrosion scales

The SEM results of corrosion scales showed acicular and spherical crystal structures which could be recognized as goethite and magnetite (Zhang et al. 2018). These crystals were found at all points, i.e., in the tube well, OHT, and distribution pipes (Fig. 4). Moreover, the microstructure of corrosion scales revealed several laminar deposits, some of which showed identical morphological resemblance with bacterial biofilm communities, though microorganisms on the sampled scale surface could have been damaged. The SEM analysis in general showed the presence of microbial colonies in scales at all the three points that have profuse interstices for the biofilm development (Fig. 4). Moreover, different types of bacteria seemed to prevail in the distribution system with rod-shaped and elongated bacteria mostly observed at tube well and OHT and filamentous bacteria in distribution pipes (Hong et al. 2010; Reyes et al. 2008; Wang et al. 2012).

### Water quality status

Water quality analysis in all the three investigated distribution systems (old and new) showed that except for Cr, Mn, and total coliform, the levels of all the physicochemical parameters were found within the WHO standards for drinking water (Table 1). Concentrations of Cr and Mn were higher at both the tube well and consumers' end and the similar trend in all the distribution systems indicated the occurrence in source water. Total coliform bacteria were present in all samples and exceeded WHO limits (5 MPN/100 ml) except for the tube well sample in DS-N2 (Table 1). Generally, in all the three systems, total coliform substantially increased in the distribution network compared to source. The presence of bacteria at source was attributable to the lack of treatment; however, in distribution systems, sewage contamination in leaking pipes as well as microbial growth due to absence of disinfection could be the main cause. Meanwhile, the abundant bacterial population in old distribution network at consumer end compared to the new system further confirmed bacterial growth in scales as observed in the SEM analysis.

**Fig. 4** SEM micrograph of corrosion scales in **a, b** tube well; **c, d** overhead tank; and **e, f** distribution pipes. Highlighted regions signify biofilms/bacteria



Although the water quality parameters were within the permissible levels, interesting trends were observed from the comparison of water quality in old and new distribution systems and the source and consumers' end using the two-way ANOVA. From the comparison of old and new pipe distribution systems, except for Cr, significant difference ( $P < 0.05$ ) was found in concentration of all the parameters (Table 2). Pairwise comparison showed that the difference was significant for alkalinity, turbidity, EC,  $\text{Cl}^-$ ,  $\text{NO}_3^-$ , pH, DO,  $\text{SiO}_4^{4-}$ , Cu, and Mn. For total hardness, significant difference of DS-O existed only with DS-N2 and for  $\text{SO}_4^{2-}$  with DS-N1. Electrical conductivity,  $\text{Cl}^-$ , Cu, and Mn were significantly higher in DS-O from both DS-N1 and DS-N2. In case of EC, the comparatively higher levels at consumers' end in DS-O caused the significant difference that may be induced by the dissolution and release of metal salts in the distribution network from scale destabilization (Makris et al. 2014). For

Cu and Mn, the higher concentration in DS-O could be traced to the occurrence in source water. In contrast, alkalinity was significantly lower from both DS-N1 and DS-N2,  $\text{SO}_4^{2-}$  from DS-N1 and total hardness from DS-N2. However, levels of these parameters were either lower from the source in DS-O (such as hardness) or variation from tube well to consumers' end (in case of alkalinity and  $\text{SO}_4^{2-}$ ) was not substantial to induce a significant change in corrosion scale characteristics.

With respect to the comparison of water quality at tube well and consumers' end in each distribution system, significant difference in general was found for turbidity,  $\text{SO}_4^{2-}$ ,  $\text{SiO}_4^{4-}$  and  $\text{Cl}^-$  (higher in tube well), and EC,  $\text{NO}_3^-$  and DO (higher at consumers' end). Turbidity was found decreasing from tube well to consumers' end in DS-N1, which indicated that suspended solids have deposited in the distribution network (Tong et al. 2016). On the contrary, turbidity increased in DS-O from source to consumers' end that pointed towards the

**Table 2** Trace heavy metals and total coliform bacteria in old and new distribution systems (SD in parenthesis)

Parameters	DS-O (old)		DS-N1 (new)		DS-N2 (new)		WHO standards
	Tube well	Consumers' end	Tube well	Consumers' end	Tube well	Consumers' end	
Chromium (mg/L)	0.51 (0.27)	0.43 (0.25)	0.31 (0.30)	0.40 (0.28)	0.31 (0.30)	0.32 (0.30)	0.05
Copper (mg/L)	2.44 (0.21)	1.80 (0.25)	1.45 (0.12)	1.47 (0.55)	1.45 (0.11)	1.49 (0.55)	2
Manganese (mg/L)	0.86 (0.00)	0.86 (0.00)	0.78 (0.01)	0.76 (0.03)	0.78 (0.01)	0.77 (0.04)	0.4
Total coliform (MPN/100 ml)	12	1070	280	635	4	9	5

mixing of corrosion residues from old pipes into the flowing water (Huang and Zhang 2005). Meanwhile, the increase in  $SO_4^{2-}$  in DS-O could be linked to a higher ratio of goethite and magnetite found in the corrosion scales (Yang et al. 2014). For  $SiO_4^{4-}$ , the pairwise comparison showed that its concentration was decreasing in DS-N1 from tube well to consumers' end but increased in DS-O. This was probably dictated by a similar trend in hardness having a direct relationship (Tong et al. 2016). Silicates have high sorption affinity for iron hydroxide and contribute to the formation of corrosion scales and different iron oxides (Davis et al. 2002). An increase in  $NO_3^-$  concentration in DS-O indicated the occurrence of nitrification process in the presence of DO (Rizk 2016). Whereas, the same in EC could have occurred due to higher  $Fe^{+2}$  concentration and decomposition of iron oxides that increases the electrical conductance (Triszcz et al. 2009). Dissolved oxygen also increased significantly in DS-O from tube well to consumers' end. Corrosion scales are known to use DO to oxidize the  $Fe^{2+}$  ion to  $Fe^{3+}$  ions and form siderite. However, as the corrosion process slows down in old systems, the concentration of DO increases (Sarin et al. 2004a). The

absence of siderite formation in the corrosion scales in distribution samples as shown in Section 3.1 also ascertained that corrosion rate has dropped resulting in lesser utilization of DO.

Moreover, the interaction effect further compared the water quality of the three distribution systems each at the source (tube well) and consumers' end from the combination effect of distribution system (new and old pipes) and specific conditions at these distribution points. Overall, the mean difference from interaction effect was significant for most of the parameters except  $SO_4^{2-}$  and heavy metals. For tube well, most of the variations seemed to mainly occur due to source water quality. The multiple pairwise comparison revealed that in tube well in DS-O, pH, Cu, and Mn were significantly higher from both DS-N1 and DS-N2, while DO from only DS-N1, whereas turbidity, hardness,  $SO_4^{2-}$ , and  $NO_3^-$  were significantly lower only from DS-N1. Likewise, at the consumer end, turbidity, EC,  $Cl^-$ , DO,  $SiO_4^{4-}$ , and Mn in DS-O were significantly higher from both DS-N1 and DS-N2 and  $NO_3^-$  from only DS-N2, while alkalinity was significantly lower from both the new systems (Table 3).

**Table 3** Two-way ANOVA for the effect of pipes in the distribution system and conditions at the tube well and consumers' end (distribution points) on water quality

Parameters	Distribution system pipes (A)		Distribution point (B)		Interaction (A × B)	
	F values	$\eta_p^2$	F values	$\eta_p^2$	F values	$\eta_p^2$
Alkalinity (mg/L)	12.4*	54%	2.9	12%	11.6*	53%
Turbidity (NTU)	79.6*	88%	6.0*	22%	193*	95%
Total Hardness (mg/L)	4.8*	31%	0.1	0.6%	8.1*	44%
EC ( $\mu S/cm$ )	7.9*	43%	12.1*	37%	6.5*	38%
pH	16.9*	62%	0.003	0.0%	19.8*	65%
$Cl^-$ (mg/L)	12.7*	55%	15.1*	42%	9.5*	48%
$SO_4^{2-}$ (mg/L)	5.7*	35%	16.1*	44%	1.2	11%
$NO_3^-$ (mg/L)	949*	99%	94*	82%	387*	97%
DO (mg/L)	53.2*	84%	11.0*	34%	17.6*	63%
$SiO_4^{4-}$ (mg/L)	95.7*	90%	8.9*	30%	228*	96%
Cr (mg/L)	62.2	6%	0.0	0.0%	19.3	2%
Cu (mg/L)	6.9*	40%	1.3	6%	1.8	15%
Mn (mg/L)	27.1*	72%	0.5	2%	0.4	4%

\*Significant at  $P < 0.05$ ;  $\eta_p^2$  = Effect size



## Conclusions

The main crystalline phases of corrosion scales in pipes were goethite, magnetite, siderite, and quartz that varied at the tube well, OHT, and consumers' end. Elemental composition showed the presence of Zn, Al, Mn, Cr, Pb, Cu, As, and Cd with Zn and Al in highest proportion at all points. The crystalline composition and elemental abundance at different points was affected by the changing water quality conditions such as DO,  $\text{Cl}^-$ ,  $\text{SiO}_4^{4-}$ ,  $\text{SO}_4^{2-}$ , EC, alkalinity, and hardness besides pipe morphological conditions. SEM micrographs of scales revealed the presence of microbial colonies resembling diatoms and elongated and filamentous bacteria. From water quality assessment, EC, Cu, and Mn in DS-O were significantly higher than in new piped systems confirming the dissolution from scales. Similarly, from source to consumers' end, turbidity, EC, DO, and  $\text{SiO}_4^{4-}$  in DS-O significantly increased ( $P < 0.05$ ) compared to new piped systems implying higher dissolution of scale residues at consumers' end and lowered corrosion rates to utilize  $\text{SiO}_4^{4-}$  and DO for iron oxidation.

**Publisher's Note** Springer Nature remains neutral with regard to jurisdictional claims in published maps and institutional affiliations.

## References

- APHA (2012) Standard methods for the examination of water and wastewater. American Public Health Association, American Water Works Association, Water Environment Federation, 22nd edn. Washington DC, USA
- Bacha AA, Durrani MI, Paracha PI (2010) Chemical characteristics of drinking water of Peshawar. *Pak J Nutr* 9:1017–1027
- Barbeau B, Carriere A, Bouchard MF (2011) Spatial and temporal variations of manganese concentrations in drinking water. *J Environ Sci Health, Pt A: Toxic/Hazard Subst Environ Eng* 46:608–616. <https://doi.org/10.1080/10934529.2011.562854>
- Barton H (2005) Predicted intake of trace elements and minerals via household drinking water by 6-year-old children from Kraków, Poland. Part 2: cadmium, 1997–2001. *Food Addit Contam* 22: 816–828. <https://doi.org/10.1080/02652030500164441>
- Benjamin MM, Sontheimer H, Leroy P (1996) Corrosion of iron and steel. Internal corrosion of water distribution systems, Cooperative Research Report, AWWA Research Foundation Denver, Co. vol 90508
- Benson AS (2009) Evaluation of iron corrosion release models for water distribution systems. Doctoral Dissertation, Virginia Tech, US
- Borch T, Camper AK, Biederman JA, Butterfield PW, Gerlach R, Amonette JE (2008) Evaluation of characterization techniques for iron pipe corrosion products and iron oxide thin films. *J Environ Eng* 134:835–844. [https://doi.org/10.1061/\(ASCE\)0733-9372\(2008\)134:10\(835\)](https://doi.org/10.1061/(ASCE)0733-9372(2008)134:10(835))
- Chaves SL, Manuel S (2013) Biofilms in drinking water: problems and solutions. *RSC Adv* 3:2520–2533. <https://doi.org/10.1039/C2RA22243D>
- Copeland RC, Lytle DA, Dionysious DD (2007) Desorption of arsenic from drinking water distribution system solids. *Environ Monit Assess* 127:523–535. <https://doi.org/10.1007/s10661-006-9299-1>
- Davis CC, Chen H-W, Edwards M (2002) Modeling silica sorption to iron hydroxide. *Environ Sci Technol* 36:582–587. <https://doi.org/10.1021/es010996t>
- Drissi SH, Refait P, Abdelmoula M, Genin JMR (1995) The preparation and thermodynamic properties of Fe (II)Fe (III) hydroxide-carbonate (green rust 1); Pourbaix diagram of iron in carbonate-containing aqueous media. *Corros Sci* 37:2025–2041. [https://doi.org/10.1016/0010-938X\(95\)00096-3](https://doi.org/10.1016/0010-938X(95)00096-3)
- Fish KE, Osborn AM, Boxall J (2016) Characterising and understanding the impact of microbial biofilms and the extracellular polymeric substance (EPS) matrix in drinking water distribution systems. *Environ Sci: Water Res Technol* 2:614–630. <https://doi.org/10.1039/C6EW00039H>
- Gonzalez S, Lopez-Roldan R, Cortina J-L (2013) Presence of metals in drinking water distribution networks due to pipe material leaching: a review. *Toxicol Environ Chem* 95:870–889. <https://doi.org/10.1080/02772248.2013.840372>
- HACH (2002) Water analysis handbook. Loveland, Colorado, USA:61–62
- Harris LJ et al (2012) A framework for developing research protocols for evaluation of microbial hazards and controls during production that pertain to the quality of agricultural water contacting fresh produce that may be consumed raw. *J Food Prot* 75:2251–2273. <https://doi.org/10.4315/0362-028X.JFP-13-007>
- Hong P-Y, Hwang C, Ling F, Andersen GL, LeChevallier MW, Liu W-T (2010) Pyrosequencing analysis of bacterial biofilm communities in water meters of a drinking water distribution system. *Appl Environ Microbiol* 76:5631–5635. <https://doi.org/10.1128/AEM.00281-10>
- Huang YH, Zhang TC (2005) Effects of dissolved oxygen on formation of corrosion products and concomitant oxygen and nitrate reduction in zero-valent iron systems with or without aqueous Fe 2+. *Water Res* 39:1751–1760. <https://doi.org/10.1016/j.watres.2005.03.002>
- Jeong Y (2005) The adsorption of arsenic (V) by iron (Fe2O3) and aluminum (Al2O3) oxides. Doctoral Dissertation, Iowa State University, US
- Khan S, Rauf R, Muhammad S, Qasim M, Din I (2016) Arsenic and heavy metals health risk assessment through drinking water consumption in the Peshawar District, Pakistan. *Hum Ecol Risk Assess Int J* 22:581–596. <https://doi.org/10.1080/10807039.2015.1083845>
- Khan S, Shahnaz M, Jehan N, Rehman S, Shah MT, Din I (2013) Drinking water quality and human health risk in Charsadda district, Pakistan. *J Clean Prod* 60:93–101. <https://doi.org/10.1016/j.jclepro.2012.02.016>
- Kim EJ, Herrera JE (2010) Characteristics of lead corrosion scales formed during drinking water distribution and their potential influence on the release of lead and other contaminants. *Environ Sci Technol* 44: 6054–6061. <https://doi.org/10.1021/es101328u>
- Li M, Liu Z, Chen Y, Hai Y (2016a) Characteristics of iron corrosion scales and water quality variations in drinking water distribution systems of different pipe materials. *Water Res* 106:593–603. <https://doi.org/10.1016/j.watres.2016.10.044>
- Li X, Wang H, Hu X, Hu C, Liao L (2016b) Characteristics of corrosion scales and biofilm in aged pipe distribution systems with switching water source. *Eng Failure Anal* 60:166–175. <https://doi.org/10.1016/j.engfailanal.2015.11.048>
- Liu G, Zhang Y, Knibbe W-J, Feng C, Liu W, Medema G, van der Meer W (2017) Potential impacts of changing supply-water quality on drinking water distribution: a review. *Water Res* 116:135–148. <https://doi.org/10.1016/j.watres.2017.03.031>
- Liu J et al (2015) Characteristics of pipe-scale in the pipes of an urban drinking water distribution system in eastern China. *Water Sci Technol Water Supply* 16:715–726. <https://doi.org/10.2166/ws.2015.183>
- Makris KC, Andra SS, Botsaris G (2014) Pipe scales and biofilms in drinking-water distribution systems: undermining finished water quality. *Crit Rev Environ Sci Technol* 44:1477–1523. <https://doi.org/10.1080/10643389.2013.790746>

- McFarland ML, Provin TL, Boellstorff DE (2008) Drinking water problems: corrosion. Texas A&M Agrilife Extension:51130–19537
- McNeill LS, Edwards M (2001) Iron pipe corrosion in distribution systems. *Am Water Works Assoc J* 93:88–100. <https://doi.org/10.1002/j.1551-8833.2001.tb09246.x>
- PBS (2017) District and Tehsil level population summary with region breakup. Pakistan Bureau of Statistics, Islamabad, Pakistan
- Peng C-Y, Korshin GV (2011) Speciation of trace inorganic contaminants in corrosion scales and deposits formed in drinking water distribution systems. *Water Res* 45:5553–5563. <https://doi.org/10.1016/j.watres.2011.08.017>
- Peng C-Y, Korshin GV, Valentine RL, Hill AS, Friedman MJ, Reiber SH (2010) Characterization of elemental and structural composition of corrosion scales and deposits formed in drinking water distribution systems. *Water Res* 44:4570–4580. <https://doi.org/10.1016/j.watres.2010.05.043>
- Reyes A, Letelier M, De la Iglesia R, Gonzalez B, Lagos G (2008) Microbiologically induced corrosion of copper pipes in low-pH water. *Int Biodeterior Biodegrad* 61:135–141. <https://doi.org/10.1016/j.ibiod.2007.06.001>
- Rizk TY (2016) Effect of nitrate treatment on corrosion, and guidelines for its implementation. *Mater Perform* 55:36–40
- Sarin P, Snoeyink V, Bebee J, Jim K, Beckett M, Kriven W, Clement J (2004a) Iron release from corroded iron pipes in drinking water distribution systems: effect of dissolved oxygen. *Water Res* 38:1259–1269. <https://doi.org/10.1016/j.watres.2003.11.022>
- Sarin P, Snoeyink V, Bebee J, Kriven W, Clement J (2001) Physico-chemical characteristics of corrosion scales in old iron pipes. *Water Res* 35:2961–2969. [https://doi.org/10.1016/S0043-1354\(00\)00591-1](https://doi.org/10.1016/S0043-1354(00)00591-1)
- Sarin P, Snoeyink V, Lytle D, Kriven W (2004b) Iron corrosion scales: model for scale growth, iron release, and colored water formation. *J Environ Eng* 130:364–373. [https://doi.org/10.1061/\(ASCE\)0733-9372\(2004\)130:4\(364\)](https://doi.org/10.1061/(ASCE)0733-9372(2004)130:4(364))
- Sedlak DL, Chan PG (1997) Reduction of hexavalent chromium by ferrous iron. *Geochim Cosmochim Acta* 61:2185–2192. [https://doi.org/10.1016/S0016-7037\(97\)00077-X](https://doi.org/10.1016/S0016-7037(97)00077-X)
- Smedley PL, Kinniburgh D (2002) A review of the source, behaviour and distribution of arsenic in natural waters. *Appl Geochem* 17:517–568. [https://doi.org/10.1016/S0883-2927\(02\)00018-5](https://doi.org/10.1016/S0883-2927(02)00018-5)
- Sun H, Shi B, Yang F, Wang D (2017) Effects of sulfate on heavy metal release from iron corrosion scales in drinking water distribution system. *Water Res* 114:69–77. <https://doi.org/10.1016/j.watres.2017.02.021>
- Tamura Y, Buduan PV, Katsura T (1981) Studies on the oxidation of iron (II) ion during the formation of Fe<sub>3</sub>O<sub>4</sub> and  $\alpha$ -FeO (OH) by air oxidation of Fe [OH]<sub>2</sub> suspensions. *J Chem Soc Dalton Trans*: 1807–1811. <https://doi.org/10.1039/DT9810001807>
- Tang Z, Hong S, Xiao W, Taylor J (2006) Characteristics of iron corrosion scales established under blending of ground, surface, and saline waters and their impacts on iron release in the pipe distribution system. *Corros Sci* 48:322–342. <https://doi.org/10.1016/j.corsci.2005.02.005>
- Tong H, Zhao P, Huang C, Zhang H, Tian Y, Li Z (2016) Development of iron release, turbidity, and dissolved silica integrated models for desalinated water in drinking water distribution systems. *Desalin Water Treat* 57:398–407. <https://doi.org/10.1080/19443994.2014.984343>
- Triszczyński JM, Porta A, Einschlag FSG (2009) Effect of operating conditions on iron corrosion rates in zero-valent iron systems for arsenic removal. *Chem Eng J* 150:431–439. <https://doi.org/10.1016/j.cej.2009.01.029>
- USAID (2014) Planning and engineering services for master plan in Peshawar Khyber Pakhtunkhwa: drinking water, sanitation/storm water and solid waste services-executive summary – Consolidation of Key Findings of Volumes 1–3 – Deliverable No. 24. USAID, Pakistan
- Veschetti E, Achene L, Ferretti E, Lucentini L, Citti G, Ottaviani M (2010) Migration of trace metals in Italian drinking waters from distribution networks. *Toxicol Environ Chem* 92:521–535. <https://doi.org/10.1080/02772240903036139>
- Wang H, Hu C, Hu X, Yang M, Qu J (2012) Effects of disinfectant and biofilm on the corrosion of cast iron pipes in a reclaimed water distribution system. *Water Res* 46:1070–1078. <https://doi.org/10.1016/j.watres.2011.12.001>
- Wang H, Hu C, Yin L, Zhang S, Liu L (2017) Characterization of chemical composition and bacterial community of corrosion scales in different drinking water distribution systems. *Environ Sci: Water Res Technol* 3:147–155. <https://doi.org/10.1039/C6EW00264A>
- Wang W-D, Yang H-W, Jiang J, Ding Z-Z, Zhu W-P (2011) Aluminum speciation in drinking water distribution system: a case study in northeastern China. *Korean J Chem Eng* 28:1227–1232. <https://doi.org/10.1007/s11814-010-0495-x>
- Yang F, Shi B, Bai Y, Sun H, Lytle DA, Wang D (2014) Effect of sulfate on the transformation of corrosion scale composition and bacterial community in cast iron water distribution pipes. *Water Res* 59:46–57. <https://doi.org/10.1016/j.watres.2014.04.003>
- Yang F, Shi B, Gu J, Wang D, Yang M (2012) Morphological and physicochemical characteristics of iron corrosion scales formed under different water source histories in a drinking water distribution system. *Water Res* 46:5423–5433. <https://doi.org/10.1016/j.watres.2012.07.031>
- Zhang H, Tian Y, Kang M, Song Y, Li H (2018) Effects of chlorination/chlorine dioxide disinfection on biofilm bacterial community and corrosion process in a reclaimed water distribution system. *Chemosphere* 215:62–73. <https://doi.org/10.1016/j.chemosphere.2018.09.181>
- Zhang Z, Stout JE, Yu VL, Vidic R (2008) Effect of pipe corrosion scales on chlorine dioxide consumption in drinking water distribution systems. *Water Res* 42:129–136. <https://doi.org/10.1016/j.watres.2007.07.054>